**Malaysian Journal of Analytical Sciences
(MJAS)**
Published by Malaysian Analytical Sciences Society

ANALIS
Persatuan Sains Analisis Malaysia

SYNTHESIS, PHOTOPHYSICAL AND COMPUTATIONAL APPROACHES ON NONLINEAR OPTICAL (NLO) PROPERTIES OF NAPHTHALEN-1-YL ETHYNYLATED-CHALCONE DERIVATIVE

(Sintesis, Pendekatan Fotofizik dan Pengkomputeran Terhadap Sifat Optik Tak Linear (NLO) bagi Terbitan Naftalen-1-il Teretinil-Kalkon)

Mas Mohammed[1], Wan M. Khairul[1]*, Rafizah Rahamathullah[2], Fazira Ilyana Abdul Razak[3], Suhaila Sapari[4]

*[1]Faculty of Science and Marine Environment,
Universiti Malaysia Terengganu, 21030, Kuala Nerus, Terengganu, Malaysia
[2]Faculty of Engineering Technology,
Universiti Malaysia Perlis, Level 1, Blok S2, Kampus UniCITI Alam, Sungai Chuchuh, 02100, Perlis, Malaysia
[3]Department of Chemistry, Faculty of Science,
Universiti Teknologi Malaysia, 81310 UTM Johor Bahru, Johor, Malaysia
[4]Department of Chemical Sciences, Faculty Science and Technology,
Universiti Kebangsaan Malaysia, 43600 UKM Bangi, Selangor, Malaysia.*

Corresponding author: wmkhairul@umt.edu.my

Abstract

A new dual mixed moieties of acetylide (C≡C) and chalcone (-CO-CH=CH) system namely 3-(naphthalen-1-yl)-1-(4-(phenylethynyl)phenyl)-2-propen-1-one (**3NPP**) was successfully designed and synthesized via Claisen Schmidt condensation reaction. Spectroscopic characterization and thermal analysis were conducted via Infrared Spectroscopy (FTIR), ^{1}H and ^{13}C Nuclear Magnetic Resonance (NMR) and Thermogravimetric (TGA) analysis. Density functional theory (DFT) assessment with basis set of B3LYP/6-31G (d,p) was computed to investigate the energy level of HOMO and LUMO, charge transfer within the molecule by global chemical reactivity descriptors (GCRD), molecular electrostatic potentials (MEP) and hyperpolarizability analyses. The simulated calculation reveals that the HOMO-LUMO energy gap of **3NPP** exhibited at 3.51 eV and has demonstrated good agreement with experimental optical band gap (E_g^{opt}). Additionally, **3NPP** possesses high NLO response with total first hyperpolarizability (β_{tot}) of 420.51×10^{-30} esu. The presence of π-conjugated acetylide groups has improved nonlinear optical property and potential for application in optoelectronic.

Keywords: ethynyl, chalcone, density functional theory, non-linear optics, first hyperpolarizability

Abstrak

Moiti dwi tercampur sistem asetilida (C≡C) dan kalkon (-CO-CH=CH) baharu yang diberi nama 3-(naftalen-1-il)-1-((4-feniletinil)fenil)-2-propen-1-on (**3NPP**) telah berjaya direkabentuk dan disintesis melalui tindak balas kondensasi Claisen Schmidt. Pencirian spektroskopi dan analisis terma telah dijalankan melalui spektroskopi inframerah (FTIR), ^{1}H dan ^{13}C Resonan Magnetik Nuklear (NMR) dan analisis termogravimetrik (TGA). Penilaian fungsi teori ketumpatan (DFT) dengan set asas

B3LYP/6-31G (d,p) telah dikira untuk mengkaji jurang tenaga bagi HOMO dan LUMO, pemindahan caj dalam sebatian melalui petunjuk kereaktifan kimia global (GCRD), potensi elektrostatik molekul (MEP) dan analisis hiperpolarisasi. Pengiraan simulasi menunjukkan jurang tenaga HOMO-LUMO **3NPP** memberikan nilai 3.51 eV dan ternyata menunjukkan nilai yang selari dengan jurang tenaga optik eksperimen (E_g^{opt}). Tambahan pula, **3NPP** mempunyai sifat NLO yang tinggi dengan jumlah hiperpolarisasi pertama (β_{tot}) sebanyak 420.51x 10^{-30} esu. Dengan kehadiran kumpulan asetilida π-terkonjugat telah meningkatkan sifat optik tak linear dan berpotensi untuk aplikasi optoelektronik.

Kata kunci: etinil, kalkon, fungsi teori ketumpatan, sifat optik tak linear, hiperpolarisasi pertama

Introduction

Recently, organic nonlinear optical (NLO) materials attracted enormous interest due to their promising applications in optical power limiting applications [1, 2], second harmonic generation (SHG) photonics and electro optic (EO) processes [3, 4]. The development of this material becomes a promising alternative approach due to their large nonlinear response, extremely fast switching time and convenient optimization routes through molecular engineering compared to the currently studied inorganic materials [5]. Among various NLO materials reported, chalcone derivatives exhibit excellent nonlinear optical (NLO) properties by having the combination of electron donor and acceptor group substituents on phenyl rings are used due to the delocalization of electron of the electron in π-conjugated system [5, 6, 7, 8]. Besides that, the process of delocalization of electron of the electron in π-conjugated leads to high electron density mobility which makes them the ideal candidates for NLO materials [9]. According to Arshad et al., Donor-π-Acceptor (D-π-A) systems are widely been used in information storage, optoelectronic, and also NLO applications. π-conjugated framework will act as the centre which gets appended by electron acceptor at one side and an electron donor group at the other side [10]. In previous study, many researchers had synthesized chalcone derivatives based on aromatic system with tuning the electron donating group (EDG) and electron withdrawing group (EWG) such as (E)-1-(4-ethylphenyl)-3-(4-(heptyloxy) phenyl) prop-2-en-1-one [11],(E)-N-(2-(3-(4-ethoxyphenyl)-1-(2-(phenyl sulfonylamine)phenyl)prop-2-en-1-one,   (E)-3-(4-chlorophenyl)-1-(2-(phenylsulfonylamine)phenyl) prop-2-en-1-one   and   (E)-3-(4-bromophenyl)-1-(2-(phenylsulfonylamine)phenyl)prop-2-en-1-one   [9].

These system were reported as the ideal candidates to be developed as NLO materials.

Within this interest, herein we present a work by introducing new chalcone-based system, 3-(naphthalen-1-yl)-1-(4-(phenylethynyl)phenyl)-2-propen-1-one (**3NPP**) with the combination of active extended conjugated acetylide system (C≡C) featuring D-π-A system. The focal point molecular candidates in this work are the extended conjugated system of acetylene (C≡C) and the chalcone system, which are made up of two distinct moieties that are used as active electronic components. Due to the extension of conjugation within the molecules aided by active donor and acceptor groups located at each terminal of the molecules, it is expected that the combination of these two systems in a single molecular framework will allow electrons to easily move through the conjugated framework from electron donor to electron acceptor group. It was designed and synthesized due to its structural simplicity and high reactivity, acetylene represents a versatile building block for organic synthesis, and its chemistry has evolved rapidly [12]. This molecule consists of π-electron which can facilitate the electron in the compound. The presence of π-conjugated polymer possessing electron-donating and electron-withdrawing groups exhibit low-lying charges transfer excited states and large second-order optical nonlinearities [13]. Besides, π-bridges and spacers, are important when tweaking NLO characteristics. The essential characteristics for a material to qualify as a good NLO material are red shifted absorption maxima, greater dipole moments, and thermal stabilities. Alkyne analogues have demonstrated blue shifted absorption maxima and worse thermal stabilities [14, 15]. In addition, the calculations were performed by using density functional theory (DFT) method to investigate

the physico-chemical properties of the designed molecule and can support experimental values. Furthermore, DFT calculation can be carried out to obtain the molecular orbitals, orbitals and electrostatic surface map [16]. In addition, DFT was used due to its great accuracy in reproducing the experimental values of molecular geometry, vibrational frequencies, atomic charges, dipole moment [17]. From the DFT calculation, NLO properties of **3NPP** can be described and compared to experimental values.

Materials and Methods

All chemicals, solvents, and reagents that were used in this work were 4-iodoacetophenone, phenylacetylene, 1-pyrenecarboxaldehyde, palladium(II) chloride, triphenylphosphine, sodium hydroxide, acetonitrile, triethylamine, tetrahydrofuran, hexane, dichloromethane, and ethanol were purchased from Acros Organics, Fisher Scientific, Merck, and Sigma Aldrich. They were used as received without further purification tasks carried out.

Characterization and Instrument

Fourier Transform-Infrared Spectrometer (ATR-FTIR) spectra were recorded using Perkin Elmer 100 spectrophotometer in the range of 4000-450 cm^{-1} spectral. The ^{1}H-NMR and ^{13}C-NMR spectroscopy analyses were conducted by using Bruker Avance III 400 MHz Spectrometer by using deuterated CDCl$_3$ as solvent. Next, the UV-Vis spectra were obtained using Spectrophotometer Shimadzu UV-1601PC in 1 cm^3 cuvette. Besides, Thermogravimetric analysis (TGA) was performed using Perkin-Elmer TGA analyzer from 30 ℃ to 900 ℃ at a heating rate of 10 ℃/min in the presence of a constant nitrogen flow.

Computational method

Frontier molecular orbitals (FMOs), global chemical reactivity descriptors (GCRD), and the NLO properties such as dipole moment, polarizability, and hyperpolarizability were carried out by density functional theory (DFT) using Gaussian 16 program package. All the images and graphs are visualized by Gauss view 6.0. The B3LYP functional was used with the 6-31G(d,p) basis set for the optimization of the structure. The basis set was chosen due to the calculated values by using B3LYP/6-31G(d,p) basis are considerably better agreement with the experimental which also includes the consideration of the polarization function supplied provided a lower error, more precise bond lengths [18].

Synthesis of precursor: 1-(4-(phenylethynyl)phenyl) ethanone (PPE)

The experimental details regard to Sonogashira precursor, **PPE** has been reported before in previous literature [19]. Hence, in this study, some modification have been carried out in for the interest of this work. 4-iodoacetophenone (0.5 g, 2.03 mmol), phenylacetylene (0.23 mL, 2.03 mmol), Pd(PPh$_3$)$_2$Cl$_2$ (40 mg, 0.057 mmol), and triethylamine (7 mL) were dissolved in tetrahydrofuran (40 mL) in the two-necked 250 mL round bottom flask. The reaction was refluxed for approximately 14 hours. The progress of the reaction was monitored by using Thin Layer Chromatography (TLC) (hexane: ethyl acetate, 4:1). After the reaction was adjudged completion, the reaction was cooled to room temperature prior filtration. Then, the mixture was dried *in-vacuo* prior purification via column chromatography to afford off-white solid as a precursor (**PPE**). Yield; 50%. The synthetic pathway of precursor is shown in Scheme 1.
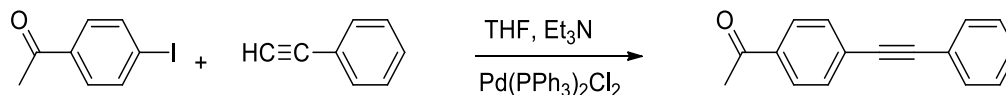

Scheme 1. Synthetic pathway for precursor, 1-(4-(phenylethynyl)phenyl)ethanone (**PPE**)

Synthesis of 3-(naphthalen-1-yl)-1-(4-(phenyl ethynyl)phenyl)-2-propen-1-one (3NPP)

The synthetic approach for the preparation of title compound (**3NPP**) is summarized in Scheme 2. 1-(4-(phenylethynyl)phenyl)ethanone (0.2 g, 0.908 mmol) was dissolved in ethanol (20 mL) in 250 mL two-necked round bottom flask. Then, 1-naphtaldehyde (0.12 mL, 0.908 mmol) was charged into the reaction while being stirred. Then, the mixture was left unattended for a few minutes in order to become homogeneous. Next, 20% sodium hydroxide solution (15 mL) was added into the

mixture dropwise and the reaction was left with constant stirring for approximately 7 hours. The progress of the reaction was monitored by using thin-layer chromatography (TLC) (hexane: dichloromethane, 3:2). After the reaction has completed, the mixture was poured into the beaker containing several ice cubes. The mixture was left overnight for the precipitate formation. After that, it was filtered and dried at ambient environment. The crude product obtained was recrystallized from acetonitrile to obtain yellow solid as the title product (yield: 75%).
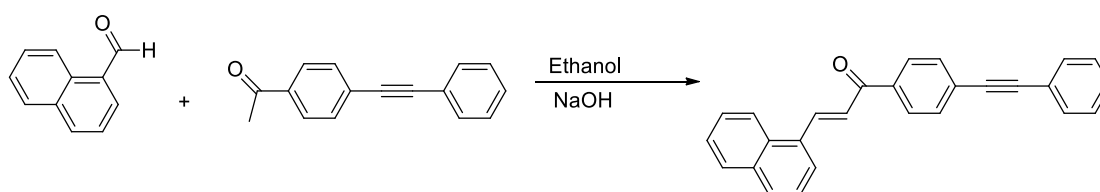
Scheme 2. Synthetic pathway for **3NPP**

Results and Discussion

Vibrational analysis

The FT-IR spectrum of **3NPP** is presented in Figure 1 within the range of 4000-450 cm^{-1}. Form the experimental data, there are five absorption bands of interest which represent the ν(CH) aromatic, ν(C≡C), ν(C=O), ν(C=C) aromatic and ν(C=C) ranging from weak to medium intensities. The absorption band for experimental stretching aromatic CH was observed at 3048 cm^{-1} and 2997 cm^{-1}. Meanwhile, the absorption band for C≡C was observed at 2361 cm^{-1} and 2342 cm^{-1} as the medium intensity peak. This peak appeared as a diminished absorption intensity of ν(C≡C) was observed due to the effect of the inter-stacking interaction and

dipole moment of the molecule [13]. The medium and sharp band for carbonyl (C=O) appeared at 1655 cm^{-1} which is supported by Mobaraki and Hemmateenejad, 2011 which stated the peak of carbonyl (C=O) stretching can be found at the range of 1750-1600 cm^{-1} [20]. In **3NPP**, the presence of intermolecular hydrogen bonds and the conjugation of the carbonyl bond with the C=C bonds greatly decrease the carbonyl group's double bond nature, lowering the stretching frequency of C=O [21]. The absorption band of C=C stretching was observed at 1589 cm^{-1} which confirms the formation of chalcone compound [22] and C=C aromatic was found at 1570 cm^{-1}.
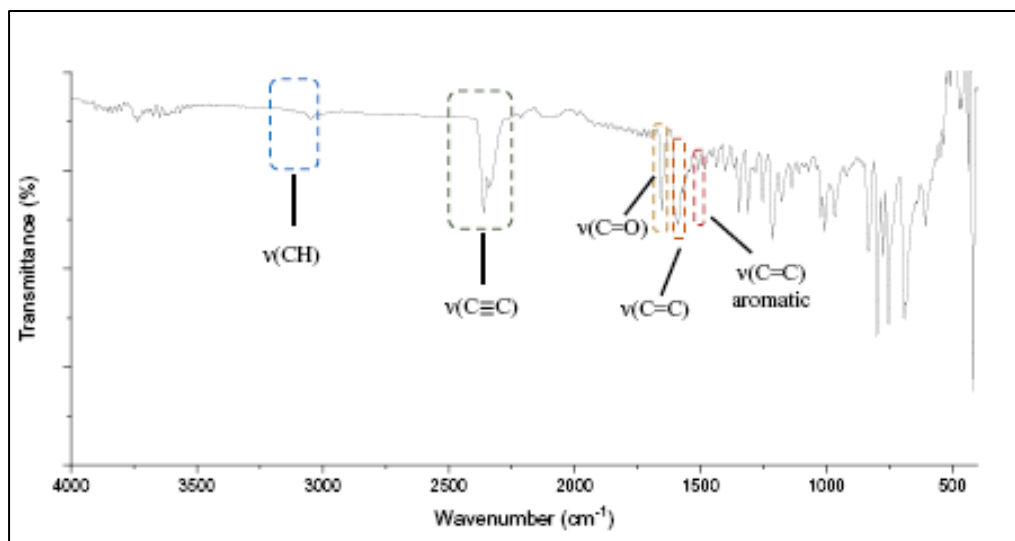
Figure 1. IR spectrum of **3NPP**

Optical properties

Electronic absorption spectrum of **3NPP** was recorded in the range of 200-600 nm in dichloromethane (DCM) solvent (c= 1×10^{-5} M). In the solution state, absorption maxima were recorded at 266 and 335 nm, which indicate π-π^* and n-π^* transitions. The value of maximum wavelength (λ_{max}) of absorption of **3NPP** was observed at 266 nm shows π-π^* transition which assigned to arise from overlapping of phenyl ring and carbonyl (C=O) chromophore. Next, n-π^* transition at the wavelength (λ_{max}) 335 nm shows the presence of carbonyl (C=O) moieties. Eq. 1 was used to calculate the optical energy band gap (E_g^{opt}), which was given in eV. According to the formula of $E_{gap} = hc/\lambda_{edge}$, the E_g value of **3NPP** is exhibited 2.92 eV.

$$E_g^{opt}(eV) = 1240 / \lambda_{edge} \qquad (1)$$

The computed electronic absorption using time dependent-DFT approach employing B3LYP functional and 6-31G (d,p) basis set in solvent effect (dichloromethane) through Integral Equation Formalism Polarizable Continuum Model (IEF-PCM). The spectrum are shown in Figure 2. The electronic transition of the computed UV-Visible at 398 nm which attributed to HOMO to LUMO transition orbitals. This region shows n-π^* and π-π^* transition which attributed the to the excitation in the aromatic ring and the presence of carbonyl (C=O) moieties [23].
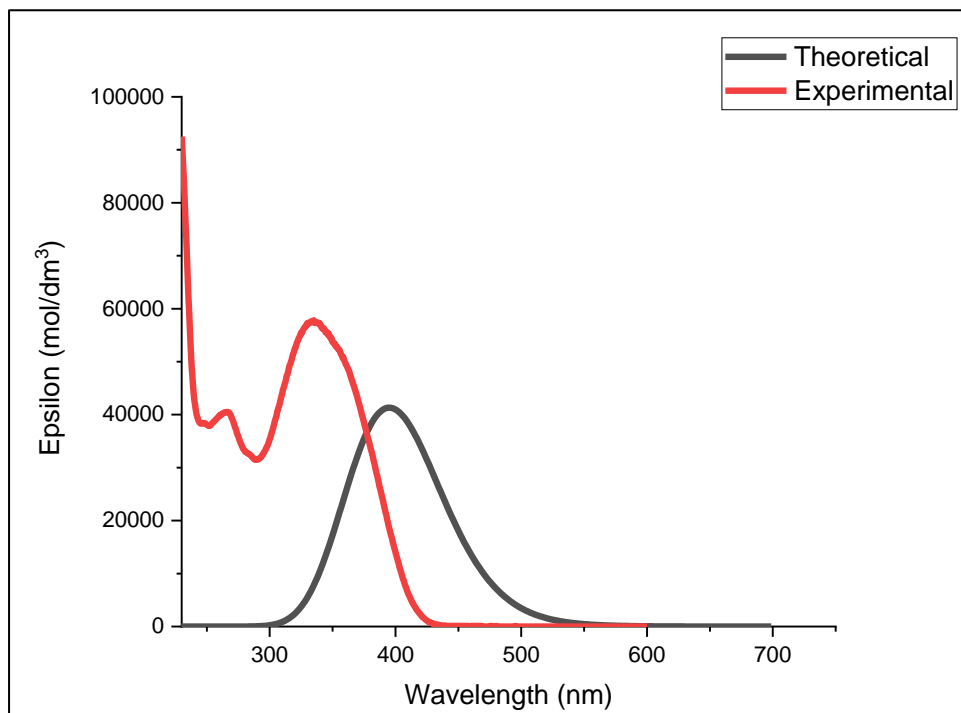
Figure 2. The UV-Visible spectrum of **3NPP**

NMR analysis

The title derivative of ethynylated-chalcone (**3NPP**) was identified by using nuclear magnetic resonance (NMR). The spectra of ^{1}H and ^{13}C NMR were recorded by using Bruker Advance III 400 spectrometer, deuterated chloroform (CDCl$_3$) is used as solvent, and trimethylsilane (TMS) was used as an internal standard. Moreover, the frequency that is used for both ^{1}H and ^{13}C NMR were 400.11 MHz and 100.61 MHz respectively. The spectra of ^{1}H and ^{13}C for **3NPP** are shown in Figure 3 and Figure 4. In ^{1}H spectrum, alkene moieties can be observed at δ_H 7.46-7.55 ppm (*J*-coupling=12 Hz) and δ_H 8.190 ppm (*J*-coupling=10 Hz) as doublet resonance multiplet due to the overlapping between the aromatic proton and doublet resonance which indicates the *E*-configuration of the synthesized compound. The strong coupling constants mostly represent the trans coupling of nearby protons, confirming the trans conformation

with regard to the double bond [24]. Then, aromatic phenyls proton which can be observed at the range of δ_H 6.900 -8.650 ppm as multiplet and pseudo-doublet resonances which are supported by previous reported studies [6].

For the ^{13}C NMR, there are two signals appeared within the range of δ_C 87.79-91.72 ppm which represent the alkyne moieties where the splitting of these peaks were due to the influence of their non-symmetrical structure [20]. The aromatic phenyls carbons can be observed at δ_C 121.54-140.71 ppm. The peak resonated at δ_C 188.25 ppm corresponded to carbonyl (C=O) carbon atom. This is due to the formation of intramolecular hydrogen bonding and electronegativity effect of oxygen atom which pulled a certain number of electrons and deshielded the resonance to higher chemical shift [20].
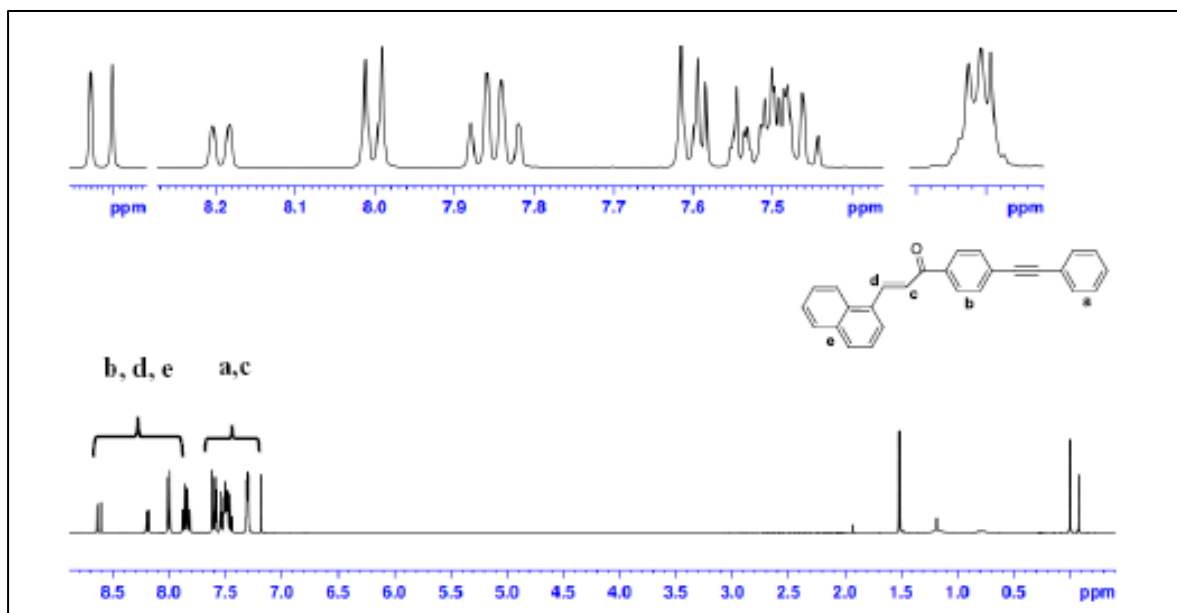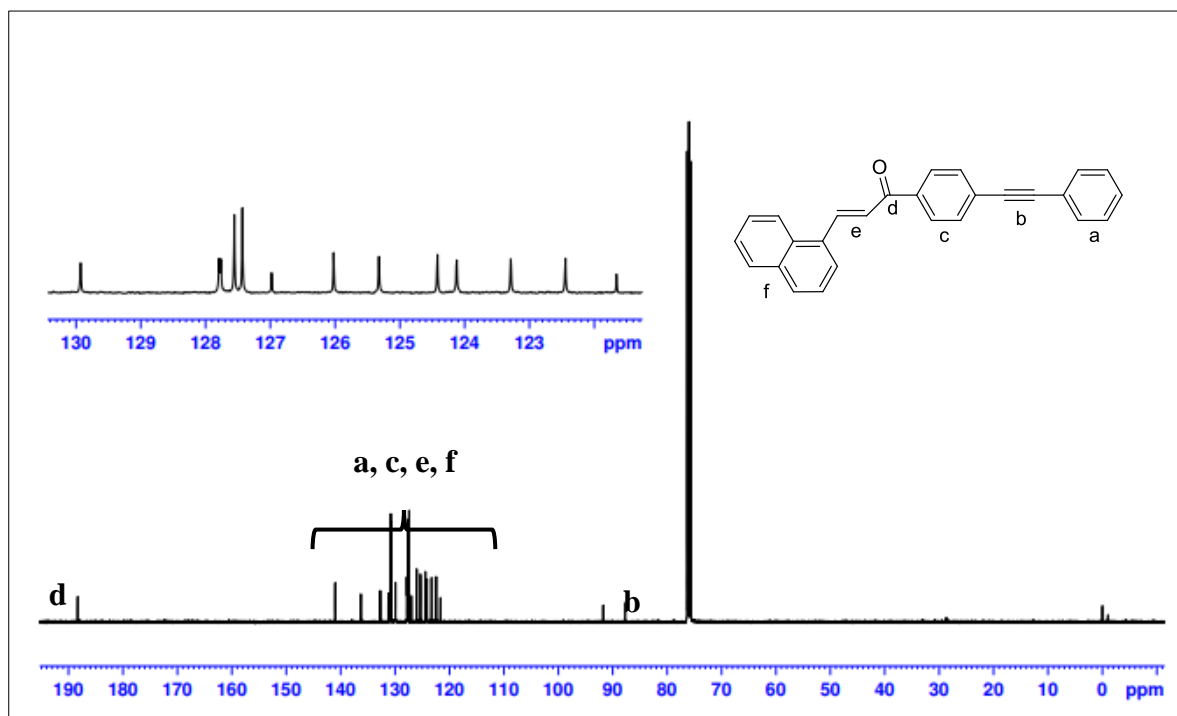
Figure 3. ^{1}H NMR spectrum of **3NPP**

Figure 4. ^{13}C NMR spectrum of **3NPP**

Thermal analysis

The TGA and DTG thermogram of **3NPP** are shown in Figure 5. The TGA/DTG curve shows that the title compound started to degrade in two steps. For the first step, the degradation occurred at 273.81 ℃ which the onset temperature (T_{onset}) and ended at 539.93 ℃ which the offset temperature (T_{offset}) with an initial weight loss of 18.27%. Meanwhile, for the second step, the degradation occurred at 539.93 ℃ which the onset temperature (T_{onset}) and stop at 735.53 ℃ which was the offset temperature (T_{offset}) with the weight loss of 72.75%. The weight loss is due to the decomposition of compound to a gaseous state. The high thermal stability of the compound is suitable for NLO application [25].
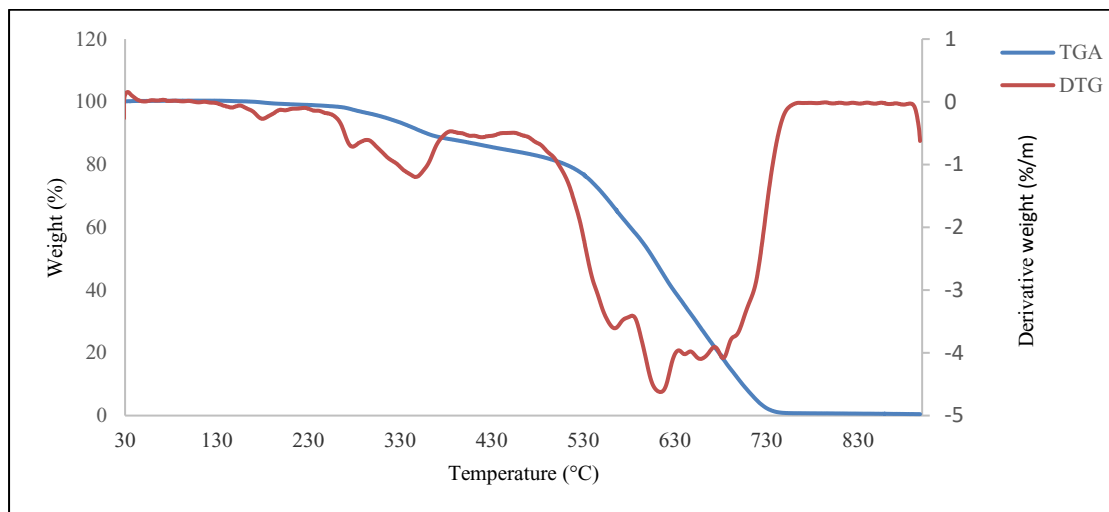

Figure 5. The TGA and DTG thermogram of **3NPP**

Frontier molecular orbitals

Frontier molecular orbitals (FMOs) are an important key role to understand the chemical stability of a molecule. The FMOs of **3NPP** was computed via TD-DFT with B3LYP/6-31G (d,p) as shown in Figure 6. The HOMO is the outermost orbital containing donor electron, while LUMO is the innermost orbital containing free places to accept electrons [16]. The HOMO is mainly concentrated on the chalcone structure and naphthalene substituent, which acts as electron donor groups. This is due to the existence of a greater electron density in the chalcone structure's naphthalene substituent. The LUMO is produced by the molecule's conjugated double bond, implying that the naphthalene substituent plays a role. Aromatic electrophile substitution reactions on chalcone structures and aromatic nucleophile substitution reactions on alkyne groups is facilitated by the naphtalene group. Furthermore, the inclusion of an alkyne group increases the title compound's intermolecular charge transfer (ICT). The energy gap for HOMO-LUMO of the synthesized molecules is relatively small which is 3.51 eV. The differences between theoretical and experimental results can be attributed to the fact that the experimental results were obtained in the solution phase, wherein various inter and intra molecule interactions can be observed within the solvent and solution. It could be attributed to a solvent phase of an isolated single molecule in theoretical calculations (using the stated software) [26]. It is found that the energy band gap relatively small than the previous chalcone compound [11]. This molecule is soft and the values of the energy bandgap is in the range of semiconducting materials which can exhibit good polarizability and non-linear optical (NLO) properties [11]. There are two electronic excitation energies were involved which are the electron transition from the ground state (S_0) to the excited state (S_n) and others information are depicted in Table 1.

Moreover, the global chemical reactivity descriptors (GCRD) are the technique to understand the chemical properties such as chemical hardness (η), chemical softness (S), chemical potential (μ), electronegativity (χ) and electrophilic index (u) = $[\mu^2/2\eta]$. The formula is derived from HOMO-LUMO energies, taking the HOMO energy as ionization potential (I) and LUMO as electron affinity (A) [27], and the data are tabulated in Table 2.

Chemical hardness (η) = $[(E_{LUMO} - E_{HOMO})/2]$ (2)
Chemical softness (S) = $[1/2\eta]$ (3)
Chemical potential (μ) = $[(E_{HOMO} + E_{LUMO})/2]$ (4)

Electronegativity (χ) = $[(I + A)/2]$ (5)
Electrophilic index (u) = $[\mu^2/2\eta]$ (6)

From the calculation, it was found that **3NPP** is kinetically stable with the hardness value of 1.76 eV, chemical potential of -4.05 eV, chemical softness of 0.28 e^{-1}V^{-1}, electronegativity of 4.05 eV and electrophilic index of 4.66 eV suggesting that the title compound gives excellent chemical strength and stability properties.
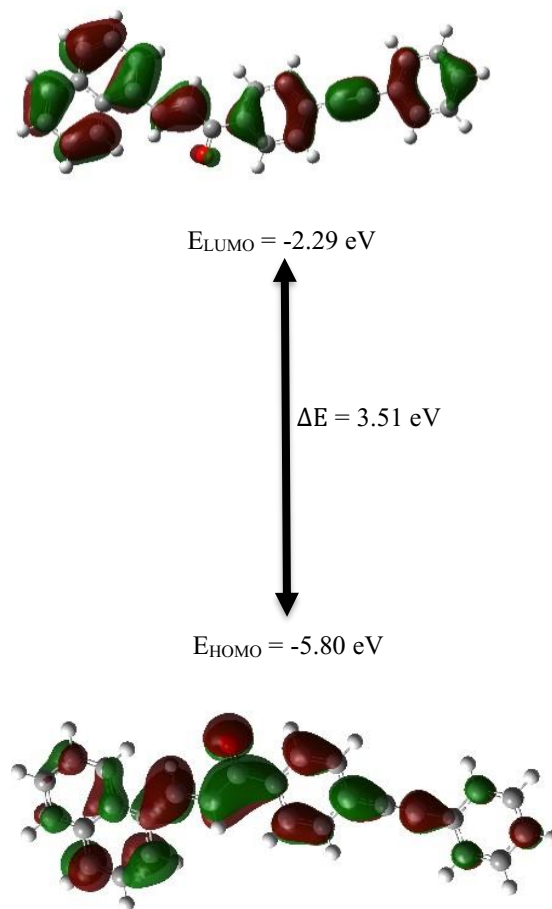

E_{LUMO} = -2.29 eV

ΔE = 3.51 eV

E_{HOMO} = -5.80 eV

Figure 6. Molecular orbitals of **3NPP**

Table 1. Excitation energy, oscillator strength and major contribution of electronic transition

Molecule	Wavelength, λ (nm)	Excitation Energy (eV)	Oscillator Strength (f_o)	Assignments, Major Contributors (%)
3NPP	403	0.07	0.67	$S_0 \rightarrow S_n$ (62.45 %)

Table 2. Molecular orbitals energies of HOMO and LUMO (eV) and the global chemical reactivity descriptors (GCRD)

Molecule	E_{HOMO}	E_{LUMO}	ΔE (eV)	η (eV)	μ (eV)	S (e^{-1}V^{-1})	χ (eV)	u (eV)
3NPP	-5.80	-2.29	3.51	1.76	-4.05	0.28	4.05	4.66

Molecular electrostatic potential analysis

The molecular electrostatic potential (MEP) analysis is computed by using DFT B3YLP/6-31G (d,p) level of theory. MEP as in Figure 7 gives important information regarding the reactive site of the molecule [28, 29], visualizing the size and shape of the molecule [30]. The reactivity of **3NPP** can be determined by predicting the nucleophile and electrophile site of the molecule. MEP surface gives the information of the charge distribution region of the molecule. In this 3D plot, the blue and brown regions indicate the positive and negative charge of **3NPP**. The blue region is spread over the hydrogen atom comprising the electrophilic sites meanwhile the red region is the nucleophilic site which contains oxygen atom [10]. For **3NPP**, the negative charges are more concentrated on the oxygen atom of the carbonyl (C=O) group in the range between -5.239×10^{-2} a.u (red) towards 5.239×10^{-2} a.u (blue) in the map because it represents a potential nucleophilic attack site. This indicates that the (C=O) oxygen atom is the most reactive spot for interacting with the nucleophile via an intermolecular hydrogen bond [6].
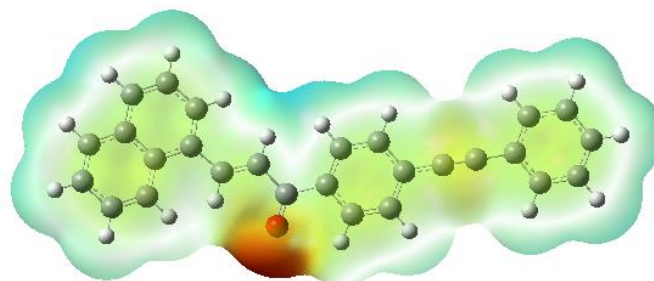

Figure 7. MEP surface for **3NPP**

Non-linear optical properties: DFT calculation

In the computational NLO studies, dynamic linear polarizabilities (α) and first hyperpolarizabilities (β) were calculated in order to examine the nonlinear optical (NLO) properties by using DFT method in the Gaussian 16 program. In addition, the isotropic polarizability ($<\alpha>$), anisotropic polarizability ($\Delta\alpha$), total beta (β_{tot}) of the first hyperpolarizability were calculated via DFT B3LYP/6-31G (d,p) and were calculated using the following equations [27, 31]. The Gaussian output file had ten hyperpolarizability tensors (β_{xxx}, β_{xyy}, β_{xzz}, β_{yyy}, β_{xxy}, β_{yzz}, β_{zzz}, β_{xxz}, β_{yyz}, β_{xyz}) and six linear polarizability tensors (α_{xx}, α_{yy}, α_{zz}, α_{xy}, α_{xz}, α_{yz})

correspondingly, in the x, y, and z directions [32]. The related parameters of **3NPP** are tabulated in Table 3.

The total dipole moment (μ_{tot}) was recorded at 2.93 which is higher than the previous chalcone compound [11]. The higher dipole moment will indicate the higher electron density which will lead to a greater charge transfer [33]. The higher the dipole moment, the higher the first polarizability will indicate the higher NLO

properties [31]. Moreover, the isotropy polarizability ($<\alpha>$) of **3NPP** was found at 57.52×10^{-24} esu, while the anisotropy of polarizability ($\Delta\alpha$) was recorded at 86.81×10^{-24} esu. Furthermore, the 1st polarizability β_{tot} of **3NPP** was 420.51×10^{-30} esu. The higher value first polarizability due to the small HOMO-LUMO gap [25].

$$\mu_{tot} = (\mu_x^2 + \mu_y^2 + \mu_z^2)^{1/2} \tag{7}$$

$$<\alpha> = \frac{1}{3}(\alpha_{xx} + \alpha_{yy} + \alpha_{zz}) \tag{8}$$

$$\Delta\alpha = \frac{1}{\sqrt{2}}[(\alpha_{xx} - \alpha_{yy})^2 + (\alpha_{yy} - \alpha_{zz})^2 + (\alpha_{zz} - \alpha_{xx})^2 + 6(\alpha_{xy}^2 + \alpha_{xz}^2 + \alpha_{yz}^2)]^{1/2} \tag{9}$$

$$\beta_{tot} = (\beta_x^2 + \beta_y^2 + \beta_z^2)^{1/2} \tag{10}$$

$$\beta_{tot} = [(\beta_{xxx} + \beta_{xyy} + \beta_{xzz})^2 + (\beta_{yyy} + \beta_{yzz} + \beta_{yxx})^2 + (\beta_{zzz} + \beta_{zxx} + \beta_{zyy})^2]^{1/2} \tag{11}$$

Table 3. Dipole moment, polarizability, and the value of 1st order hyperpolarizability

Dipole moment (Debye)	3NPP
μ_{tot}	2.93
Polarizability, α ($\times 10^{-24}$ esu)	
α_{xx}	110.17
α_{yy}	18.40
α_{zz}	44.00
α_{xy}	-8.81
α_{xz}	11.67
α_{yz}	7.45
$<\alpha>$ ($\times 10^{-24}$) in esu	57.52
$\Delta\alpha$ ($\times 10^{-24}$) in esu	86.81
1st Hyperpolarizability, β ($\times 10^{-30}$ esu)	
β_{xxx}	-102.36
β_{xyy}	2.53
β_{xzz}	-9.28
β_x	-342.06
β_{yyy}	0.40
β_{xxy}	14.75
β_{yzz}	1.48
β_y	53.09
β_{zzz}	-1.18
β_{xxz}	-72.76
β_{yyz}	-9.46
β_z	238.75
β_{xyz}	8.90
β_{tot}	420.51

Conclusion

The new conjugated ethynylated based chalcone (**3NPP**) featuring D-π-A concept was designed and successfully synthesised as active non-linear optical (NLO) response. From the findings, the title compound of **3NPP** is thermally stable up to 320.60 ℃ with the weight loss of 91.02 % in two steps of degradation process. The introduction of acetylide moiety reveals the enhancement of stability of this system. The energy band gap of **3NPP** is 3.51 eV which is compatible to further this system for optoelectronics applications. According to the findings, this compound also could be used as a good NLO active material. The development of suitable electron transport materials for organic electronic devices can be aided by precise design, synthesis, and theoretical investigation of these compounds. Furthermore, the molecular electrostatic potential (MEP) also shows the reactive sites in this reaction. **3NPP** also has excellent NLO properties by DFT calculation with the value of β_{tot} =420.51× 10^{-30} esu and reveals good polarizability. From the preliminary outcome, further investigation on the similar molecular system can be applied as ideal and promising NLO material for the development of any optical application.

Acknowledgment

References

1. Sankaraperumal, A., Shetty, A. N. and Karthikeyan, J. (2015). Structural characterization and nonlinear optical properties of 1-phenyl-3-(4-bis(2-chloroethyl)aminophenyl)-2-propen-1-one. *Journal of Structural Chemistry*, 56: 1398-1404.

2. Abegão, L. M. G., Fonseca, R. D., Santos, F. A., Souza, G. B., Barreiros, A. L. B. S., Barreiros, M. L., Alencar, M. A. R. C., Mendonca, C. R., Silva, D. L., Boni, L. D. and Rodrigues Jr, J. J. (2016). Second- and third-order nonlinear optical properties of unsubstitutedand mono-substituted chalcones. *Chemical Physical Letters*, 648: 91-96.

3. Shkir, M., Riscob, B. and Bhagavannarayana, G. (2012). Synthesis, growth, structural, spectroscopic, crystalline perfection, second harmonic generation (SHG) and thermal studies of 2-aminopyridinium picrate (2APP): A new nonlinear optical material. *Solid State Sciences*, 14(7): 773-776.

4. Liu, J., Ouyang, C., Huo, F., He, W. and Cao, A. (2020). Progress in the enhancement of electro-optic coefficients and orientation stability for organic second-order nonlinear optical materials. *Dyes and Pigments*, 181: 108509.

5. Prasad, A. A., Muthu, K., Meenatchi, V., Rajasekar, M., Agilandeshwari, R., Meena, K., Manonmoni, J. V. and Meenakshisundaram, S. P. (2015). Optical, vibrational, NBO, first-order molecular hyperpolarizability and hirshfeld surface analysis of a nonlinear optical chalcone. *Spectrochimica Acta Part A: Molecular and Biomolecular Spectroscopy*, 140: 311-327.

6. Ekbote, A., Patil, P. S., Maidur, S. R., Chia, T. S. and Quah, C. K. (2017). Structural, third-order optical nonlinearities and figures of merit of (e)-1-(3-substituted phenyl)-3-(4-fluorophenyl)prop-2-en-1-one under CW regime: New chalcone derivatives for optical limiting applications. *Dyes and Pigments*, 16: S0143-7208.

7. Zaini, M. F., Khairul, W. M., Arshad, S., Abdullah, M., Zainuri, D. A., Rahamathullah, R., Rosli, M. I., Aziz, M. S. A. and Razak, I. A. (2020). The structure-property studies and mechanism of optical limiting action of methyl 4-((4-aminophenyl)ethynyl)benzoate crystal under continuous wave laser excitation. *Optical Materials*, 107: 110087.

8. Ganapayya, B., Jayarama, A., Sankoli, R., Hathwar, V. R. and Dharmaprakash, S. M. (2012). Synthesis, growth, and characterization of a new NLO material 3-(2,3-Dimethoxyphenyl)-1-(pyridin-2-yl)prop-2-en-1-one. *Journal of Molecular Structure*, 1007: 175-178.

9. Patil, P. S., Gummagol, N. B., Ekbote, A., Wong, Q. A., Quah, C. K., Shkir, M., Maidur, S. R. and Rao, S. V. (2020). Structural and femtosecond third-order nonlinear optical properties of electron donor-acceptor substituted chalcones: an experimental and computational approach. *Journal of Molecular Structure*, 1219: 128523.

10. Custodio, J. M. F., Gotardo, F., Vaz, W. F., D'Oliveira, G. D. C., de Almeida, L. R., Fonseca, R. D., Cocca, L. H. Z., Perez, C. N., Oliver, A. G., de Boni, L. and Napolitano, H. B. (2020). Benzenesulfonyl incorporated chalcones: synthesis, structural and optical properties. *Journal of Molecular Structure*, 1208: 127845.

11. Arshad, M. N., Al-Dies, A, M., Asiri, A. M., Khalid, M., Birinji, A. S., Al-Amry, K. A. and Braga, A. A. C. (2017). Synthesis, crystal structures, spectroscopic and nonlinear optical properties of chalcone derivatives: a combined experimental and theoretical study. *Journal of Molecular Structure,* 1141: 124-156.

12. Daud, A. I., Khairul, W. M., Augustine, E., Arshad, S. and Razak, I. A. (2019). Synthesis, spectroscopic, structural elucidation, NLO characteristic and hirshfeld surface analysis of (e)-1-(4-ethylphenyl)-3-(4-(heptyloxy)phenyl)prop-2-en-1-one: a dual approach of experimental and DFT calculations. *Journal of Molecular Structure*, 1194: 124-137.

13. Voronin, V. V., Ledovskaya, M. S., Bogashenkov, A. S., Rodygin, K. S. and Ananikov, V. P. (2018). Acetylene in organic synthesis: recent progress and new uses. *Molecules*, 23: 2442.

14. Sakaguchi, T., Azuma, S. and Hashimoto, T. (2016). Metathesis polymerization of diphenylacetylenes possessing electron-donating and electron-withdrawing groups and emission properties of polymers. *Synthetic Metals*, 212: 174-179.

15. Moylan, C. R., Twieg, R. J., Lee, V.Y., Swanson, S. A., Betterton, K. M. and Miller, R. D. (1993). Nonlinear optical chromophores with large hyperpolarizabilities and enhanced thermal stabilities. *Journal of the American Chemical Society*, 115: 12599-12600.

16. Ghanavathar, C. W., Mishra, V. R. and Sekar, N. (2021). Review of NLO phoric azo dyes – developments in hyperpolarizabilities in last two decades. *Dyes and Pigments*, 191: 109367.

17. Teixeira, A. M. R., Santos, H. S., Bandeira, P. N., Juliao, M. S. S., Freire, P. T. C., Lima, V. N., Cruz, B. G., da Silva, P. T., Coutinho, H. D. M. and Sena Jr, D. M. (2019). Structural, spectroscopic and microbiological characterization of the chalcone 2e-1-(2′-hydroxy-3′,4′,6′-trimethoxyphenyl)-3-(phenyl)-prop-2-en-1-one derived from the natural product 2-hydroxy-3,4,6-trimethoxyacetophenone. *Journal of Molecular Structure*, 1179: 739-748.

18. Kosar, B. and Albayak, C. (2011). Spectroscopic investigations and quantum chemical computational study of (e)-4-methoxy-2-[(p-tolylimino)methyl]phenol. *Spectrochimica Acta Part A: Molecular and Biomolecular Spectroscopy*, 78: 160-167.

19. Boudhar, K., Debieche, M., Serhane, A. and Zeghdaoui, A. (2021). Crystal structure, raman spectroscopy study and quantum chemical DFT calculations of n-phenyl -3-para nitro phenyl isoxazolidine-5-carbonitrile. *Journal of Molecular Structure*, 1246: 131029.

20. Thorand, S. and Krause, N. (1998). Improved procedures for the palladium-catalyzed coupling of terminal alkynes with aryl bromides (sonogashira coupling). *Journal of Organic Chemistry*, 1998: 8551-8553.

21. Mobaraki, N. and Hemmateenejad, B. (2011). Structural characterization of carbonyl compounds by IR spectroscopy and chemometrics data analysis. *Chemometrics and Intelligent Laboratory Systems*, 109: 171-177.

22. John, J. S., Sajan, D., Narayana, C., Joy, N. and Philip, R. (2018). Theoretical and experimental approach to the investigation of hyperpolarizability and charge transfer characteristics of NLO active 2′,3,4,4′,5-pentamethoxy chalcone with silver atoms adsorbed. *Optical Materials*, 84: 409-421.

23. Prabu, S. R., Upadhyaya, V. and Jayarama, A. (2017). Synthesis, crystal structure and hirshfeld surface analysis of a novel chalcone derivative: (*2e*)-3-(2,3-dimethoxyphenyl)-1-(3-nitrophenyl) prop-2-en-1-one. *Chemical Data Collections*, 11-12: 199-210.

24. Khairul, W. M., Zuki, H. M., Hasan, M. F. A. and Daud, A. I. (2016). Pyridine acyl thiourea as ionophore for the detection of copper (II) in aqueous phase. *Procedia Chemistry*, 20: 105-114.

25. Kumar, P. C. R., Ravindrachary, V., Janardhana, K., Manjunath, H. R., Karegouda, P., Crasta, V. and Sridhar, M. A. (2011). Optical and structural properties of chalcone NLO single crystals. *Journal of Molecular Structure*, 1005: 1-7.

26. Naik, V. S., Patil, P. S., Gummagol, N. B., Wong, Q. A., Quah, C. K. and Jayanna, H. S. (2020). Structural, linear optical, second and third-order nonlinear optical properties of two halogenated chalcone derivatives containing thiophene moiety. *Chemical Physics Letters*, 761: 138051.

27. Pramod, A. G., Nadaf, Y. F. and Renuka, C. G. (2019). A combined experimental theoretical approach for energy gap determination, photophysical, photostable, optoelectronic, NLO, and organic light emitting diode (OLED) application: synthesized coumarin derivative. *Journal of Molecular Structure*, 1194: 271-283.

28. Maidur, S. R., Patil, P. S., Rao, S. V., Shkir, M. and Dharmaprakash, S. M. (2017). Experimental and computational studies on second- and third-order nonlinear optical properties of a novel D-p-A type chalcone derivative: 3-(4-methoxyphenyl)-1-(4-nitrophenyl) prop-2-en-1-one. *Optics and Laser technology*, 97: 219-228.

29. Zaini, M. F., Razak, I. A., Khairul, W. K. and Arshad, S. (2020). Structural, Hirshfeld and DFT studies of conjugated D–π–A carbazole chalcone crystal. *Crystallographic Communications*, E76: 387-391.

30. Barakat, A., Al-Majid, A. M., Soliman, S. M., Mabkhot, Y. N., Ali, M., Ghabbour, H. A., Fun, H-K. and Wadood, A. (2015). Structural and spectral investigations of the recently synthesized chalcone (*E*)-3-mesityl-1-(naphthalen-2-yl) prop-2-en-1-one, a potential chemotherapeutic agent. *Chemistry Central Journal*, 9: 35.

31. Anizaim, A. H., Arshad, S., Zaini, M. F., Abdullah, M., Zainuri, D. A. and Razak, I. A. (2019). Third order nonlinear optical properties of selected fluorinated chalcone derivatives. *Optical Materials*, 98: 109406.

32. Woon, P. S., Sapari, S., Matmin, J. and Razak, F. I. A. (2020). Computational studies on nonlinear optical properties of metal complexes containing azobenzene. *Malaysian Journal of Analytical Sciences*, 24: 719-726.

33. Khalid, M., Ali, A., Jawaria, R., Asghar, M. A., Asim, S., Khan, M. U., Hussain, R., ur Rehman, M. F., Ennis, C. J. and Akram, M. S. (2020). First principles study of electronic and nonlinear optical properties of A–D–π–A and D–A–D–π–A configured compounds containing novel quinoline–carbazole derivatives. *RSC Advances*, 10: 22273.

34. Bartashevich, E. and Tsirelson, V. (2013). Atomic dipole polarization in charge-transfer complexes with halogen bonding. *Physical Chemistry Chemical Physics*, 15: 2530-2538.